

Significant performance improvement in polarization-diversity GMSK reception using atypical filters

Ádám Kiss, and László Schäffer

Abstract—This paper presents novel signal processing methods to enhance the reception performance of Gaussian Minimum Shift Keying (GMSK) signals from pico- and nanosatellites, emphasizing software-defined approaches over hardware upgrades. Atypical filtering techniques, including phase-domain median and FIR filtering, as well as polarization-diverse multi-channel methods, are explored and evaluated. Real-world experiments were conducted using coherently sampled dual-polarization channels from a ground station in Szeged, Hungary, receiving transmissions from the MRC-100 satellite. Various single- and multi-channel preprocessing strategies were benchmarked using packet decoding success and bit-error rates. Results show that non-linear phase filtering and blind source separation techniques, notably FastICA, significantly increase the number of correctly decoded packets – achieving up to a 16% improvement compared to conventional demodulation without preprocessing. This study demonstrates the utility and relative independence of these methods and highlights their potential for improving satellite data throughput with no hardware modification. These techniques are suitable for integration into existing ground stations to enhance data reception performance.

Index Terms—CubeSat, GMSK, Independent Component Analysis, Median filter, PocketQube, Polarization-diversity.

I. INTRODUCTION

SEVERAL approaches are available for transferring data from a space satellite. Yet, the most notable example is the use of radio signals, particularly sub-gigahertz frequencies, in educational and research satellites. One classic, widely used modulation is Gaussian Minimum Shift Keying (GMSK) [1] on the 70 cm radio amateur band and on the industrial satellite band on slightly lower frequencies. The typical effective radiated power is 100 mW, with an average path loss of around 150 dB. To ensure a reliable transmission, a robust error-correcting method and sufficient signal levels are required. If a specific satellite is already in orbit, the only way to increase the data rate is to build a better reception architecture. Although one possible improvement of the ground station is to enhance antenna dimensions and optimize filter characteristics, realizing these are not cost-efficient. The primary motivation of this research was to identify and analyze receiver algorithms that enhance nano- and pico-satellite reception without requiring an investment in a more expensive reception system. To the best of our knowledge, no published results are using such non-linear filters to improve GMSK reception. The Independent Component Analysis (ICA) algorithm was used for separating parallel transmissions [2], [3], [4]. However, utilizing it to select the desired signal from a noisy environment is poorly covered.

Department of Technical Informatics, University of Szeged, Hungary
Corresponding author: Ádám Kiss (e-mail: kissadam@inf.u-szeged.hu).

DOI: 10.36244/ICJ.2025.4.4

In this paper, following a brief introduction to the measurement setup, some non-linear methods are introduced in Section III to preprocess the radio signals, which only require a single channel as input. A separate section –numbered IV—presents methods operating on two coherently sampled, independent channels. As we aim to enlarge the size of downloaded data, we quantitatively compare the number of successfully decoded correct packets and qualitatively compare the bit-error rate of the same packet among methods. Every comparison is shown with the reference state-of-the-art GMSK demodulator. On amateur radio bands, it is common to conduct experiments like this to investigate radio channel performance. [5] Therefore, we have chosen a satellite operating on these bands.

II. MEASUREMENT SETUP

The experiments presented in this paper were conducted in the central area of Szeged, Hungary, in an environment where TV and FM broadcast transmitters, along with various cellular base stations, loaded the receiver input in addition to the useful signal. Generally, the presence of such strong signals can easily overload the input amplifier of a radio receiver to a non-linear domain. Therefore, the pre-selected radio filters like the one below should be used.

The actual measurements were made in the 70 cm radio amateur band, with the radio tuned to the MRC-100 [6] satellite, which operates at 436.72 MHz. This satellite was chosen because a reliable, coherent, soft-decision, state-of-the-art GMSK demodulator software called “smogcl2” [7] is compatible with it, which can also output the bit-error ratio of the demodulated packets.

The front of the reception chain consisted of two linear 10-element Yagi-Uda antennas, each with a 30-degree-wide main lobe. These antennas were mounted perpendicularly to each other, so their main lobes pointed in the same direction, but their linear polarization planes were orthogonal to each other.

In addition to differences in polarization, the two signal paths exhibited variation in their hardware stages, specifically through the incorporation of distinct filters. One polarization plane’s path (designated as “Channel A”) included only a Surface Acoustic Wave (SAW) filter, followed by a low noise amplifier. The other path (designated as “Channel B”) consisted of a low-Q, low insertion loss cavity filter, a low insertion loss SAW filter, and the same low-noise amplifier. Both signal paths were terminated in a software-defined radio configured to a coherent sampling rate of 1 MHz.

All the antennas were mounted onto an antenna rotator with a positioning accuracy of approximately ten degrees. It was controlled by software named “Gpredict” [8] using the solutions of Kepler-equations provided by a space tracking service, namely the North American Aerospace Defense Command (NORAD). [9] The rotator was stepped in five degrees.

Other aspects of the reception is presented in [10].

After input filtering, Doppler correction was performed coherently on both channels using the data from NORAD. We should note that, theoretically, the correction could be done without the exact trajectory data. [11] The data were then resampled and saved at a sample rate of 50 kHz, suitable for processing with “smogcli2”. The length of specific windows should also be related to this symbol rate. It is essential to note that the satellite sent various packets at different baud rates. In this research, packets sent at a rate of 12500 bauds were only considered in the Results section, as they were dominant during the operation of the MRC-100.

Various methods are investigated, encompassing a wide range of diverse scenarios. The IQ output of each scenario was processed using “smogcli2”. Alongside the packets, the corresponding bit-error ratios were recorded.

To provide a reference for comparing the proposed non-linear polarization-diversity methods, several linear and single-channel techniques were also evaluated. The signal processing procedures run in 0.8-second-long overlapped windows, stepped in a raster of 0.2 seconds. Shorter windows resulted in the loss of certain packets even if the experimental procedures studied herein were omitted. In contrast to this, if longer windows had been applied, the incoherence of the reception would have increased (phase incoherency occurring from the change of the angle of incidence).

III. SINGLE-CHANNEL METHODS

In the case of single-channel methods, only one signal path was considered, and the two signal paths were not combined in any way to mutually improve reception quality.

The word “band limiting” in this article references a kind of filtering, which was always performed in the single-channel methods. A Finite Impulse Response (FIR) filter with a 12 kHz cut-off frequency was applied, designed with a 3 kHz transition band using Blackman-window [12]. The bandwidth of such a filter was 24 kHz in the complex spectrum, which included most of the 12500 baud GMSK signal power [1], taking into account also the possible inaccuracy of the Doppler correction.

A. Channel A and Channel B

These cases represent the raw received packets without any preprocessing.

B. Channel data with median filtered phase

This case is a non-linear method, running on a band-limited channel and acting on the phase of the recorded IQ signals. The amplitude of the IQ signal remains unchanged, but its unwrapped phase is median filtered [13] using 3, 5,

or 7 sample-wide windows. The window sizes were chosen to fit the trivial median definition; therefore, only odd, wide windows were used. Windows wider than four samples – corresponding to durations longer than a single symbol – begin to introduce intersymbol interference, which gradually leads to a decline in performance. Windows longer than 7 samples were omitted in this study.

In terms of mathematics

$$|Out[k]| = |Input[k]| \quad (1)$$

$$j = \frac{N-1}{2} \quad (2)$$

$$\arg(Out[k]) = \text{Median}_{i=k-j}^{k+j} \arg(Input[i]) \quad (3)$$

Where N is the length of the filter, k is the time dimension, and \arg is the unwrapped phase of its argument.

C. Channel data with FIR filtered phase

This case is also a non-linear method, running on a band-limited channel and acting on the phase of the recorded IQ signals like in the “Channel data with median filtered phase” case, but this time, the unwrapped phase is FIR filtered by 3, 5, or 7 sample wide rectangle-shaped windows with unity gain.

In terms of mathematics, using equation 1 and 2:

$$\arg(Out[k]) = \sum_{i=k-j}^{k+j} \frac{1}{N} \arg(Input[i]) \quad (4)$$

IV. MULTI-CHANNEL METHODS

In the case of the multi-channel methods, the two available, coherently sampled, diverse signal paths were combined using different methods.

A. Averaging Channel A and Channel B

In this case, the IQ data of the two channels are averaged sample by sample. Assuming that the same signal is on both channels, this increases the signal-to-noise ratio. This case is essentially equivalent to stacking Yagi-Uda antennas [14], a common practice in satellite tracking ground stations.

In terms of mathematics

$$Out[k] = ChannelA[k] + ChannelB[k] \quad (5)$$

B. Averaging Channel A and Channel B with path correction

In this paper, path correction refers to a phase correction that aligns the phase of channel B with that of channel A, thereby maximizing the average output amplitude of the sum of the two channels.

In this case, the sum of the two channels after the path correction forms the output.

In terms of mathematics

$$Out[k] = ChannelA[k] + ChannelBC[k] \quad (6)$$

Where $ChannelBC$ is rotated in phase to have the highest correlation with $ChannelA$.

C. Averaging Channel A and Channel B in the quadrature-amplitude space

Averaging is not only applicable to the IQ form of the signal but also to its amplitude and phase. Aimed to investigate its effect, the two channels are averaged separately by their amplitudes and phases.

In terms of mathematics

$$|Out[k]| = |ChannelA[k]| + |ChannelB[k]| \quad (7)$$

$$\arg Out[k] = \arg(\exp^{j \arg ChA[k]} + \exp^{j \arg ChB[k]}) \quad (8)$$

D. Median filtered phase of the averaged signals

In this case, the two band-limited and path-corrected channels are averaged sample by sample. The amplitudes remain intact, while the phase of the averaged signals is median-filtered by three and five sample-wide median filters.

Essentially, this entire case represents a concatenation of methods IV-B and III-B.

E. Independent Component Analysis

In earlier solutions, blind source separation techniques have been used on GMSK signals in Automatic Identification Systems [2], [3] and multi-input multi-output systems [4].

In this case, the band-limited and path-corrected IQ signals are converted to an intermediate frequency, producing real signals for each channel. These real signals are processed with the FastICA [15] algorithm, which separates the original signals into a non-gaussian component with the highest variance and an additional residual component, both of which are treated as output.

F. Independent Component Analysis with median filtered phase

In this case, the output of the FastICA algorithm is downconverted to zero intermediate frequency again, and the quadrature components of the results are median filtered with three and five sample wide windows (as in case III-B).

V. RESULTS

The results were examined by both the number of successfully decoded packets and the bit-error rate of them. Venn diagrams were created to visualize the independence and performance of the algorithms based on the found packets. The algorithms were compared by the bit-error rate of the simultaneously found packets with the aid of correlograms. A 23-day observation of the MRC-100 satellite signals was conducted for evaluation, collected between October 21, 2023, and November 12, 2023. [16]

The results can be interpreted both quantitatively and qualitatively. We can measure how many packets with good checksums the demodulator found after the bit-error correction and investigate whether an algorithm found much more CRC-correct data in a raw radio recording than other algorithms. Furthermore, we should also note if an algorithm has found not as many data packets as others, but a significant number of them is unique among the listed methods. On the other hand,

we can compare specific methods by examining the quality (in terms of the bit-error rate) of commonly found packets using correlograms.

We used the FastICA implementation in Scikit-Learn 1.6.0 [17] with the default parameters. The random seed was set to 42 to ensure reproducibility.

A. Single-input methods

According to the Venn diagrams [18], no unique packets were found when the 5- and 7-bin moving average FIR filter was applied to the phase. To enhance the readability of Fig. 1, they were omitted.

Fig. 1 shows that most of the packets uniquely found by these methods resulted from the median filtering of the unwrapped phase with three and five sample-wide windows. Using those algorithms, the number of packets increases by 101 on Channel A (4.3% increase relative to demodulating only the raw data) and by 101 on Channel B (3.7% increase relative to demodulating only the raw data).

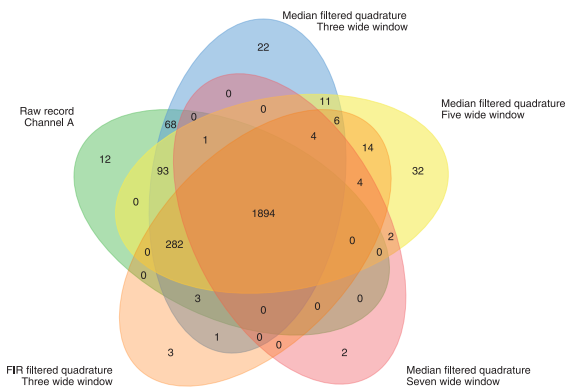


Fig. 1. Comparison of single-input methods on recordings. The number inside each bubble represents the number of packets detected using the corresponding method. 101 of 2453 packets were missed without the proposed methods.

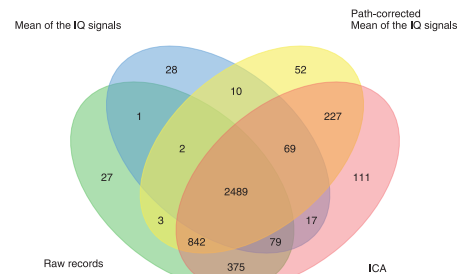


Fig. 2. Comparison of multi-input linear methods. 215 of 4322 packets were missed when only the raw radio signal recordings were considered.

B. Multiple input methods

Fig. 2 shows a significant number of unique packets (514, 13.5% relative increase to demodulating only the raw data

on the two channels) when using the following methods: averaging the IQ signals, averaging the path-corrected IQ signals, and the ICA.

Fig. 3 shows that median filtering the phase on the averaged IQ signals, median filtering the phase of the ICA results, and quadrature averaging methods also significantly increase the number of packets (551, 14.4% increase relative to demodulating only the raw data on the two channels).

The summary of the highlighted methods is shown in Fig. 4. The group “single channel methods” include the raw recordings and the filtered phase raw recordings. The group “mean like methods” covers the addition of the two signals and the path-corrected addition of the two signals. The group “quadrature-oriented methods” includes the quadrature-amplitude averaging method with and without a phase median filter on its output. 10.7% of the packets were missed without the proposed multi-path methods related to the cumulated performance of raw recordings and the single-channel methods.

The Venn diagrams show the number of packets detected by these methods from the raw recordings and measure their contribution to the amount of data downloaded. There are several packets that appear as a result of multiple decoding methods, these can be compared by their quality. One objective measure of the quality is the bit-error ratio.

Fig. 5 and 6 show correlations [19] between the bit-error ratio of the commonly decoded packets. Co-decoded packets, mainly scattered near the equal performance line, suggest that the two methods strongly correlate in terms of bit-error ratios. If most of the packets deviate below the equal performance line, then we can conclude that co-decoded packets exhibit a lower bit-error rate on the vertical axis. Therefore, comparing the co-decoded packets, the method labeled horizontally (in the row) outperforms the one labeled vertically (in the column).

The cumulative gain of these algorithms is 611 packets (16% relative to the packets from the non-preprocessed recordings). The Venn diagram and the correlograms both show that these methods are partly independent.

C. Processing time

The implementation was done in NumPy [20] environment. For one – approximately 10 minutes long – pass of the MRC-100 satellite, evaluation of all the listed methods took an hour

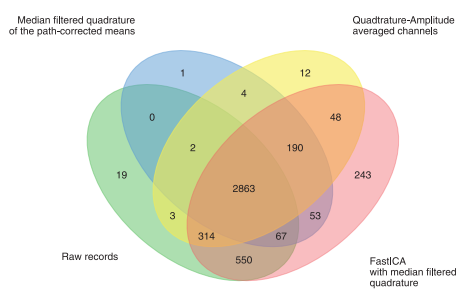


Fig. 3. Comparison of multi-input phase filtering methods. 551 of 4369 packets were missed without the proposed methods.

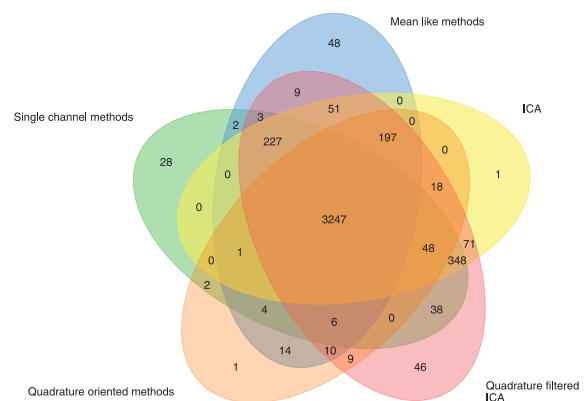


Fig. 4. Comparison of all presented methods. The number inside each bubble represents the number of packets detected using the corresponding method groups. Numerous packets are found only by different methods, furthermore these methods are partly independent.

on a standard desktop computer (i7-9700KF, 30 GiB RAM), which was less than the revisit period. Preliminary tests show that by utilizing parallel computation methods (such as GPUs), quasi-real-time operation is achievable.

VI. DISCUSSION

The results allow us to evaluate the effectiveness of various methods and compare their performance. The Venn diagrams highlight that a significant number of packets were detected and successfully decoded exclusively by the proposed methods. Using the bit-error-rate correlograms, we can analyze the performance of multiple methods on the common packets. If there is no correlation between the bit-error rates, we can infer that the algorithms were practical under different scenarios. Conversely, a high correlation would suggest that the two methods perform with similar efficiency. Additionally, correlograms where points fall consistently above or below the equal bit-error-ratio line indicate that one method outperforms the other in terms of bit-error rate.

As Fig. 5 shows, the seven bin wide windows underperformed the other methods according to bit-error-ratios. Also, Fig. 1 shows that only two new data packets were detected using the seven-wide filters. This further suggests that more than five wide windows could be omitted, most probably due to intersymbol interference.

Although single-channel algorithms are easy to implement in software-defined radio systems, the now-rare hardware radios might need further adjustments or upgrades. Applying multichannel methods to polarity-diverse reception stations with coherent sampling radio is also straightforward.

VII. CONCLUSION

In this paper, we investigated the performance of different atypical filters in a real environment on GMSK signals from space. Furthermore, we introduced and compared trivial and non-trivial polarization diversity methods. The FastICA algorithm and median filtering of signal phases are highly adaptable for use in diverse reception systems and recommended for

Significant performance improvement in polarization-diversity GMSK reception using atypical filters

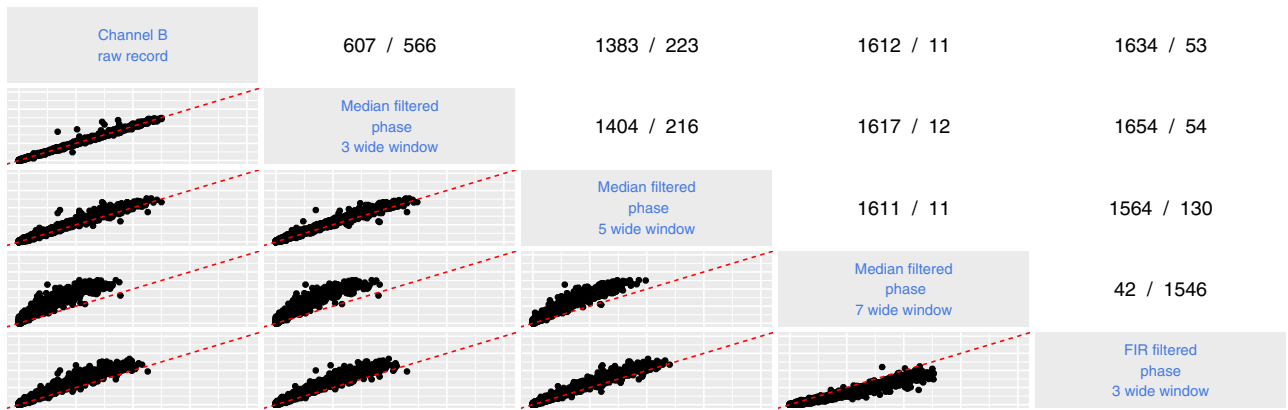


Fig. 5. Correlation between the bit-error rate in different single-input methods. The vertical and horizontal scales range from 0 to 20% on every subgraph, indicating the bit-error ratio. The horizontal axis is labeled along the same column; the vertical axis is labeled along the same row. A dashed equal-performance line is plotted for reference. The bottom-left corner contains the packets without bit error. This shows that the three sample long median filtering does not alter the BER for the co-found packets. The upper triangle shows how many co-found packets have better BER in the method named along the row (first number) and how many are named along the column (second number).

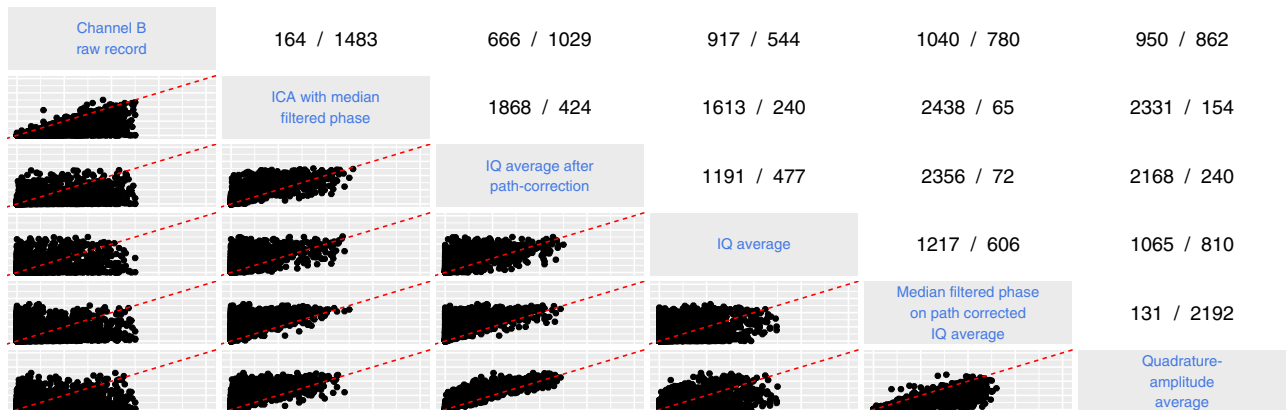


Fig. 6. Correlation between the bit-error-rate in different multi-input methods. Square-like scatter plot indicates independency, while triangle like ones indicate better BER using one method than the other.

adaptation in existing systems. While ICA effectively covers the problem of multi-antenna receptions as a clear use case, the underlying mechanism of median filtering is less clear and requires further research. Other algorithms were also found to be useful, though less effective. With sufficient processing time, a ground station could apply all these methods to the received signals to gather more data. In the future, other blind source separation algorithms, such as JADE or Infomax, should be considered and compared. In summary, implementing these techniques significantly increased the volume of data downloaded in the system by 16% as described above. These algorithms (especially the single-channel ones) can be easily implemented and integrated on GMSK receiver sites to increase downloading performance.

ACKNOWLEDGMENT

The reception system supplying the data for this research was provided by IKIKK, Centre of Excellence for Interdisciplinary Research, Development and Innovation of the University of Szeged, and Csiha Innovation and Technology Plc., Szeged, Hungary.

The research was supported by project TKP2021-NVA-09, which has been implemented with the support provided by the Ministry of Innovation and Technology of Hungary from the National Research, Development and Innovation Fund, financed under the TKP2021-NVA funding scheme.

REFERENCES

- [1] K. Murota and K. Hirade, "GMSK modulation for digital mobile radio telephony," *IRE Trans. Commun. Syst.*, vol. 29, no. 7, pp. 1044–1050, Jul. 1981. **DOI:** 10.1109/TCOM.1981.1095089.
- [2] "A steady FastICA algorithm based on modified-m estimate function," in *Proceedings of 2016 the 6th International Workshop on Computer Science and Engineering, WCSE*, 2016. **DOI:** 10.18178/wcse.2016.06.026.
- [3] A. Krishna, A. Nimbal, A. Makam A, and V. Sambasiva Rao, "Implementation of fast independent component analysis on field-programmable gate array for resolving the slot collision issue in the space-based automatic identification system," en, *Int. J. Satell. Commun. Netw.*, vol. 38, no. 6, pp. 480–498, Nov. 2020. **DOI:** 10.1002/sat.1362.
- [4] M. Yu, C. Li, B. Xu, and Y. Li, "GMSK modulated DSSS signal separation based on principal component analysis," in *2020 IEEE 20th International Conference on Communication Technology (ICCT)*, Nanning, China: IEEE, Oct. 2020. **DOI:** 10.1109/ICCT50939.2020.9295670.
- [5] E. Laport, E. Tilton, and R. Rowe, "Amateur radio," *IEEE Communications Magazine*, vol. 19, no. 4, pp. 16–24, 1981. **DOI:** 10.1109/MCOM.1981.1090543.
- [6] Y. A. I. Humad and L. Dudás, "Resonant radar reflector on vhf / uhf band based on bpsk modulation at leo orbit by mrc-100 satellite," *Infocommunications journal*, vol. 16, no. 1, pp. 26–34, 2024, ISSN: 2061-2079. **DOI:** 10.36244/icj.2024.1.4. [Online]. Available: <http://dx.doi.org/10.36244/ICJ.2024.1.4>.
- [7] M. Maroti and P. Horváth, Smogli2, 2023. **DOI:** 10.5281/zenodo.10207615.
- [8] A. R. Periyapatna et al., "Automation of a satellite earth station," in *2023 IEEE 8th International Conference for Convergence in Technology (I2CT)*, Lonavla, India: IEEE, Apr. 2023, pp. 1–6. **DOI:** 10.1109/I2CT57861.2023.10126424.
- [9] S. Speretta, P. Sundaramoorthy, and E. Gill, "Long-term performance analysis of norad two-line elements for cubesats and pocketqubes," Apr. 2017.
- [10] Á. Kiss, A. Tönköly, and R. Mingesz, "Descriptor: Thermal sensor comparison on the mrc-100 satellite (mrc100szte)," *IEEE Data Descriptions*, pp. 1–9, 2025. **DOI:** 10.1109/IEEEDETA.2025.3624344.
- [11] T. Herman and L. Dudás, "Picosatellite identification and doppler estimation using passive radar techniques," *Infocommunications Journal*, vol. 15, no. 3, pp. 11–17, 2023, ISSN: 2061-2079. **DOI:** 10.36244/icj.2023.3.2. [Online]. Available: <http://dx.doi.org/10.36244/ICJ.2023.3.2>.
- [12] S. Chakraborty, "Advantages of blackman window over hamming window method for designing fir filter," *International Journal of Computer Science & Engineering Technology*, vol. 4, no. 08, 2013. [Online]. Available: <https://api.semanticscholar.org/CorpusID:14186524>.
- [13] B. I. Justusson, "Median filtering: Statistical properties," in *Topics in Applied Physics*, Berlin/Heidelberg: Springer-Verlag, 2006, pp. 161–196. **DOI:** 10.1007/BFb0057597.
- [14] L. Dudas, L. Papay, and R. Seller, "Automated and remote controlled ground station of masat-1, the first hungarian satellite," in *2014 24th International Conference Radioelektronika*, Bratislava, Slovakia: IEEE, Apr. 2014. **DOI:** 10.1109/Radioelek.2014.6828410.
- [15] A. Hyvärinen and E. Oja, "Independent component analysis: Algorithms and applications," en, *Neural Netw.*, vol. 13, no. 4-5, pp. 411–430, May 2000. **DOI:** 10.1016/s0893-6080(00)00026-5.
- [16] Á. Kiss, Doppler-corrected iq signals from the mrc-100 satellite, 2024. **DOI:** 10.21227/8mr2-jw13.
- [17] F. Pedregosa et al., "Scikit-learn: Machine learning in Python," *Journal of Machine Learning Research*, vol. 12, pp. 2825–2830, 2011.
- [18] J. D. Hunter, "Matplotlib: A 2d graphics environment," *Computing in science & engineering*, vol. 9, no. 03, pp. 90–95, 2007.
- [19] J. W. Emerson et al., "The generalized pairs plot," en, *J. Comput. Graph. Stat.*, vol. 22, no. 1, pp. 79–91, Jan. 2013. **DOI:** 10.1080/10618600.2012.694762.
- [20] C. R. Harris et al., "Array programming with NumPy," *Nature*, vol. 585, no. 7825, pp. 357–362, Sep. 2020. **DOI:** 10.1038/s41586-020-2649-2. [Online]. Available: <https://doi.org/10.1038/s41586-020-2649-2>.



Ádám Kiss is a PhD student at the Department of Physiology, University of Szeged. He earned his degree in electrical engineering, specializing in telecommunications, from the Budapest University of Technology and Economics. His research focuses primarily on physiological signal processing and radio communications.



László Schäffer obtained his B.Sc. degree in engineering information technology in 2013, his M.Sc. degree in computer science and technology in 2015, and his PhD in computer science in 2022 from University of Szeged. Currently he is an assistant professor at the Department of Technical Informatics, University of Szeged. His research interests include FPGA based prototype development, real-time neurophysiological and digital signal processing, and embedded systems.